


RESEARCH ARTICLE

Nanoliposome C6-Ceramide in combination with anti-CTLA4 antibody improves anti-tumor immunity in hepatocellular cancer

Xiaoqiang Qi¹ | Feng Wu¹ | Sung Hoon Kim¹ | Jussuf T. Kaifi^{1,2} | Eric T. Kimchi^{1,2} | Helena Snyder³ | Anuradha Illendula³ | Todd Fox³ | Mark Kester³ | Kevin F. Staveley-O'Carroll^{1,2} | Guangfu Li^{1,2,4} 

¹Department of Surgery, University of Missouri-Columbia, Columbia, Missouri, USA

²Ellis Fischel Cancer Center, University of Missouri-Columbia, Columbia, Missouri, USA

³Department of Pharmacology, University of Virginia, Charlottesville, Virginia, USA

⁴Department of Molecular Microbiology and Immunology, University of Missouri-Columbia, Columbia, Missouri, USA

Correspondence

Kevin F. Staveley-O'Carroll,
Department of Surgery, School of
Medicine, University of Missouri, One
Hospital Dr., Columbia, MO 65212,
USA.

Email: ocarrollk@health.missouri.edu

Guangfu Li, Department of Surgery,
Molecular Microbiology and
Immunology, Ellis Fischel Cancer
Center, University of Missouri-
Columbia, Roy Blunt NextGen
Precision Health Building, Room 2002,
1030 Hitt Street, Columbia, MO 65212,
USA.

Email: liguan@health.missouri.edu

Funding information

R01CA208396 (Guangfu Li, Mark
Kester, Kevin F. Staveley-O'Carroll),
R01 CA250536 (Guangfu Li, Kevin F.

Abstract

Combination therapy represents an effective therapeutic approach to overcome hepatocellular cancer (HCC) resistance to immune checkpoint blockade (ICB). Based upon previous work demonstrating that nanoliposome C6-ceramide (LipC6) not only induces HCC apoptosis but also prevents HCC-induced immune tolerance, we now investigate the potential of LipC6 in combination with ICB in HCC treatment. We generated orthotopic HCC-bearing mice, which have typical features in common with human patients, and then treated them with LipC6 in combination with the antibodies (Abs) for programmed cell death protein 1 (PD-1) or cytotoxic T-lymphocyte antigen 4 (CTLA4). The tumor growth was monitored by magnetic resonance imaging (MRI) and the intrahepatic immune profiles were checked by flow cytometry in response to the treatments. Realtime PCR (qPCR) was used to detect the expression of target genes. The results show that LipC6 in combination with anti-CTLA4 Ab, but not anti-PD-1 Ab, significantly slowed tumor growth, enhanced tumor-infiltrating CD8⁺ T cells, and

Abbreviations: Abs, Antibodies; ACUC, Animal Care and Use Committee; ADCP, antibody dependent cellular phagocytosis; α PD-1 Ab, anti-PD-1 antibody; CCl₄, Carbon tetrachloride; CTLA-4, cytotoxic T-lymphocyte-associated protein 4; DCs, dendritic cells; EPR, enhanced permeability and retention; FDA, Food and Drug Administration; FoxP3, forkhead box protein P3; HCC, hepatocellular cancer; ICB, immune checkpoint blockade; ICI, immune checkpoint inhibitor; ICT, Immune checkpoint therapy; IP, intraperitoneal; IV, intravenous; ISPL, intrasplenic; KLF2, Krüppel-like Factor 2; LipC6, nanoliposome C6-ceramide; MRI, magnetic resonance imaging; NCI, National Cancer Institute; PD-1, programmed cell death protein 1; PFS, progression-free survival; qPCR, Real-time PCR; RTKI, multiple receptor tyrosine kinase inhibitor; RFA, Radiofrequency ablation; SOR, Sorafenib; scRNA-seq, single-cell RNA sequencing; TAg, SV40 T antigen; TSA, tumor-specific antigen; TIL, tumor-infiltrating leukocyte; TAM, tumor associated macrophage; WT, wild-type.

Xiaoqiang Qi and Feng Wu contributed equally to this work and share the first authorship.

This is an open access article under the terms of the Creative Commons Attribution-NonCommercial-NoDerivs License, which permits use and distribution in any medium, provided the original work is properly cited, the use is non-commercial and no modifications or adaptations are made.

© 2022 The Authors. *The FASEB Journal* published by Wiley Periodicals LLC on behalf of Federation of American Societies for Experimental Biology

Staveley-O'Carroll), I01 BX004065 (Eric Kimchi, Kevin Staveley-O'Carroll), and Ellis Fischel Cancer Center Pilot Project Grant (Guangfu Li)

suppressed tumor-resident CD4⁺CD25⁺FoxP3⁺ Tregs. Further molecular investigation indicates that the combinational treatment suppressed transcriptional factor Krüppel-like Factor 2 (KLF2), forkhead box protein P3 (FoxP3), and CTLA4. Our studies suggest that LipC6 in combination with anti-CTLA4 Ab represents a novel therapeutic approach with significant potential in activating anti-HCC immune response and suppressing HCC growth.

KEYWORDS

hepatocellular cancer (HCC), immune checkpoint blockade (ICB), Krüppel-like Factor 2 (KLF2), nanoliposome C6-ceramide (LipC6)

1 | INTRODUCTION

Hepatocellular cancer (HCC) is the only cancer in the United States with an incidence that continues to rise. It is estimated there will be more than 1 million new cases in 2025.^{1,2} Lack of effective therapies makes HCC the third-highest cause of cancer-related death.^{3–5} Surgical resection and liver transplantation are curative treatments, but only suitable for a small number of early-stage patients.^{6,7} Other clinically feasible non-surgical and non-transplant-based therapies provide limited benefit.^{8–11} Sorafenib (SOR), a multiple receptor tyrosine kinase inhibitor (RTKI), is the first FDA-approved chemotherapy to treat HCC, but only increases median lifespan by less than 3 months.^{1,12} Although immune checkpoint inhibitors (ICIs)-based cancer immunotherapy has shown unprecedented and durable clinical response in a wide range of tumor types,^{13,14} the reported overall objective response rate of human patients with HCC to anti-programmed death-1 antibody (α PD-1 Ab) is only 14%.¹⁵ A press release by Bristol Myers Squibb on July 26, 2021, indicates that nivolumab (monoclonal α PD-1 Ab) as a single agent for the treatment of HCC patients previously treated with SOR has been withdrawn from the US market. Thus, there is an urgent need in developing novel therapeutic approaches to improve immune checkpoint treatment against HCC.

The lack of a clinically relevant animal model for HCC represents a critical barrier in understanding HCC immunity and developing immunotherapeutic strategies. To overcome this limitation, we have established a clinically relevant murine model which mimics the typical biological and immunological features of human HCC.^{16,17} In this unique model, androgen production in the recipient mice drives the expression of SV40 T antigen (TAg) specifically in transplanted hepatocytes under the control of the liver-specific major urinary protein promoter. As a result, oncogenic TAg production induces the spontaneous transition of transplanted hepatocytes to cancer. Therefore, TAg functions as a tumor-specific antigen (TSA) in this model, which allows us to study TSA immune response

during tumor initiation and progression. This unique model has been successfully utilized to elucidate mechanisms underlying tumor-induced immunotolerance toward the development of novel therapeutic approaches against HCC.¹⁸ Considering 80% to 90% of clinical cases,¹⁹ HCC occurs in the setting of fibrosis, we treat mice with CCl₄ to induce liver fibrosis prior to ISPL inoculation of oncogenic hepatocytes. As a result, HCC initiates to grow in the context of liver fibrosis.^{16,17,20,21} Both models reflect the typical features of human disease in biology and immunology. The HCC mice without CCl₄-induced liver fibrosis were used in this study, we have detected the increased gene expression of tumor-associated genes in the tumors, including *Afp* and *Gpc3* (Figure S1).

Ceramides are a family of lipid molecules consisting of sphingosine and a fatty acid.^{17,22} It is referred to as a “tumor suppressor lipid” since it powerfully mediates different signaling events including apoptosis, cell cycle arrest, and autophagic response.^{23,24} Using nanotechnology, we prepared nanoliposome-loaded C6-ceramide (LipC6) and demonstrated that this nano-formula LipC6 overcomes biochemical barriers and allows C6-ceramide to travel through the bloodstream and target tumor cells through enhanced permeability and retention (EPR).²² Most importantly, we demonstrated that LipC6 not only inhibits tumor growth but also breaks immune tolerance. The combination of LipC6 and immunotherapy destroys established HCC tumors.¹⁷ We, and the National Cancer Institute (NCI) Nanotechnology Characterization Laboratory, have completed the extensive preclinical evaluation to characterize the physical/chemical, toxicological, and pharmacokinetic properties of LipC6, as well as its safety and therapeutic potential in cancer treatment,²⁵ potentially facilitating its clinical use as a drug.²⁶ A phase 1 clinical trial (NCT#02834611) has recently been completed with no dose-limiting toxicities and stable disease observed in just under 50% of the treated patients.

The potential of LipC6 in suppressing HCC growth and preventing HCC-induced immunotolerance encourages

us to explore whether LipC6 can improve ICB for HCC by their combination. In this study, we evaluate the therapeutic efficacy of LipC6-based integration with α PD-1 Ab or anti-cytotoxic T-lymphocyte antigen 4 antibody (α CTLA4 Ab) on HCC in our unique murine model. The results demonstrate that the combination of LipC6 with α CTLA4 Ab, but not α PD-1 Ab, significantly slows tumor growth through activating tumor-infiltrating CD8⁺ T cells and suppressing tumor-resident CD4⁺CD25⁺FoxP3⁺ Tregs. Further mechanistic studies indicate that LipC6-mediated expressional suppression of CTLA4 and transcriptional factor Krüppel-like Factor 2 (KLF2) in tumor-infiltrating CD8⁺ T cells contributes to effector CD8⁺ T cell activation.

2 | MATERIALS AND METHODS

2.1 | Murine model of HCC

Line MTD2 mice served as the source of tumorigenic hepatocytes and were maintained by our laboratory.²⁷ Male C57BL/6 mice were purchased from Jackson Laboratory (Bar Harbor, ME) and used as recipients in preparation for the HCC tumor model.¹⁸ All experiments involving animals were performed under the protocol approved by the Animal Care and Use Committee (ACUC) of the University of Missouri. All the mice received humane care according to the criteria outlined in the “Guide for the Care and Use of Laboratory Animals”.

The orthotopic murine model was developed by seeding TAg-transgenic hepatocytes isolated from young male MTD2 mice into the livers of C57BL/6 mice by intrasplenic (ISPL) inoculation with our established protocol.¹⁶ Briefly, C57BL/6 mice under general anesthesia with isoflurane underwent a 0.5 cm flank incision. Spleen was exposed and placed two 10 mm titanium clips between the upper and lower branch of the splenic vasculature, then the spleen was cut between two clips. Hepatocytes were injected into the lower pole of the spleen and flowed into the liver through the portal vein. A third clip was placed on the lower branch of the vascular pedicle and the lower pole of the spleen was removed. The abdominal wall was sutured with 5-0 VICRYL suture.

2.2 | MRI for monitoring tumor growth

Tumor surveillance was conducted with MRI in a small animal imaging center at Harry S. Truman Memorial Veteran's Hospital.^{17,28} All MRI scans were obtained on a 7.0 Tesla system (Bruker Biospin, Billerica, MA) with

in-plane resolution 0.1 mm and slice thickness 1 mm. Mice were anesthetized with isoflurane inhalation and the vital signs were monitored throughout imaging. Abdominal T₂-weighted (T₂W) MRI was acquired for tumor volume measurements.

2.3 | Treatments with α PD-1 Ab, α CTLA4 Ab, and LipC6

α PD-1 Ab (CAT# BE0146, BioXCell, USA), α CTLA4 Ab (CAT# BE0131, BioXCell, USA), or their IgG isotypes (CAT# BE0089, CAT# BE0087, BioXCell, USA) were intraperitoneally injected into mice every 3 days for two weeks at 100 μ g/mouse in 200 μ l of PBS buffer. LipC6 or its ghost control (nanoliposome without ceramide) were administered to mice via intravenous injection every other day for 2 weeks at 35 mg/kg body weight in 200 μ l volume.

2.4 | Isolation of tumor-infiltrating leukocytes

Mice were anesthetized with isoflurane, then underwent liver/tumor perfusion via portal vein with 15 ml of 0.05% collagenase (Gibco, Gaithersburg, MD) in Ca²⁺-free PBS at a pump speed of 4 ml/min. After perfusion, livers or tumors were harvested, cut to small pieces, and incubated in 0.04% collagenase in GBSS (Sigma, St. Louis, MO) for 20 min at 37°C with shaking at 240 rpm for the entire digestion. Samples underwent the filter through a 250 μ m mesh, lower speed of centrifugation, RBC lysis, wash with GBSS. The resultant cell pellet was suspended in 15 ml of GBSS plus 18.45 ml 30% Nycodenz solution (Accurate Chemical & Scientific Inc., Westbury, NY), and centrifuged at 1400 g for 20 min at room temperature with a setting of no-brake. Liver or tumor-infiltrating leukocytes enriched in the top layer were collected and washed twice with RPMI 1640 complete medium.¹⁷

2.5 | Ex vivo stimulation of liver/tumor-infiltrating leukocytes with TSA peptides

Splenocytes, liver/tumor-infiltrating leukocytes were freshly isolated, suspended, and cultured in RPMI 1640 complete medium (Gibco, Gaithersburg, MD) at 37°C in a 5% CO₂ humidified atmosphere. The cells were stimulated with TSA epitope peptides or control peptides at a dose of 1 μ M for 5 h in the presence of 3 μ g/ml of Brefeldin A (Biolegend, San Diego, CA) which prevents cytokine secretion.

2.6 | In vitro culture of splenic cells and purified pan T cells

Spleens were harvested from male wild-type C57BL/6 mice, then smashed in RPMI 1640 complete medium (Gibco, Gaithersburg, MD). Splenic cells were passed through a 40 μm mesh filter (Fisherbrand, Canada), harvested cell pellet by centrifugation, then incubated in RBC lysis buffer (BD Pharm Lyse) for 5 min at 37°C to remove red blood cells. Pan T cells were purified from splenic cells via Pan T cell Isolation Kit II (CAT#130-095-130, Miltenyi Biotec, US) according to the manufacturer's instruction. The prepared splenic cells or purified pan T cells were cultured in RPMI 1640 complete medium at 37°C in a 5% CO₂ humidified atmosphere with indicated treatment.

For in vitro cell assay, 1×10^6 mixed splenocytes or purified pan T cells were seeded into a 12-well plate, then treated with 10 $\mu\text{g}/\text{ml}$ αCTLA4 Ab or 10 μM LipC6. 24 h later, the cells were harvested for flow cytometry or qPCR analysis.

2.7 | siRNA transfection for Klf2 knockdown

Purified pan T cells were seeded into 12-well plates at a density of 1×10^6 cells/well, then received the transfection of siRNA for Klf2 (CAT#SR411977A, OriGene Technologies Inc. Rockville, US) or scrambled siRNA (CAT#SR30004, OriGene Technologies Inc., Rockville, US) at a dose of 20 nM with Lipofectamine[®] RNAiMAX transfection reagent (CAT#13778150, Invitrogen, Waltham, US) according to the manufacturer's recommended procedures. 24 h post-transfection, cells were harvested for cellular experiments.

2.8 | Flow cytometric analysis

Ex vivo staining of lymphocytes from spleens and tumors with fluorochrome-labeled Abs was performed on a single-cell suspensions as described.¹⁸ Stained cells were analyzed with a Fantasia X20 flow cytometer (BD Biosciences, San Jose, CA). Data were analyzed using the FlowJo software (Tree Star, Ashland, OR). Staining of intracellular IFN- γ , FoxP3 and KLF2 was performed with intracellular/intranuclear protein buffer set (Thermo Fisher Scientific, Waltham, MA) following the manufacturer's instruction. Fluorochrome-labeled Abs for CD3 (CAT#100236), CD8 (CAT#100748), CD4 (CAT#100438), CD45 (CAT#147708), CD69 (CAT#104530), CD25 (CAT#101908), NK 1.1 (CAT#156507) and CD49b (CAT#103515) Abs were

purchased from BioLegend (San Diego, US); Abs for IFN- γ (CAT#12-7311-82), FoxP3 (CAT#12-4774-42) and CTLA4 (CAT#12-1522-82) were purchased from Thermo Fisher Scientific (Waltham, MA); and Abs for KLF2 (CAT#orb9120) was purchased from Biorbyt Inc. (Cambridge, UK).

2.9 | Immunohistochemical staining (IHC)

Liver or tumor tissues were fixed with 10% neutral buffered formalin and embedded in paraffin. Tissue sections were processed to conduct IHC. Briefly, tissue sections were de-paraffinized with xylene, rehydrated with various grades of ethanol (100%, 95%, 80%, and 70%), unmasked for antigen retrieval with the provided solution (Vector Laboratories Inc., Burlingame, CA), permeabilized with 0.2% Triton X-100, blocked with serum, and then incubated with BLOXALL reagent (Vector Laboratories Inc., Burlingame, CA) to quench endogenous peroxidase. Subsequently, the sections were incubated in succession with primary antibodies, secondary antibodies, and DAB substrate at the optimized concentration to develop color. The positive cells were counted in 5 randomly selected fields in each slide with ImageJ software (National Institutes of Health, Bethesda, MD). Abs for cleaved caspase 3 Ab (CAT#9964S), cleaved PARP Ab (CAT#94885S), and CD8a Ab (CAT#98941S) were purchased from Cell Signaling Technology (Danvers, USA), and respectively used for marking the apoptosis cells and effector CD8 T cells.

2.10 | Real-time PCR (qPCR)

Tissues were homogenized by Pellet Pestles (Kontes, Vineland, NJ). Total RNAs were extracted with RNeasy[®] Micro kit (Qiagen, Germantown, MD). Reverse transcription of RNA to cDNA was conducted with the High-Capacity cDNA Reverse Transcription kit (Applied Biosystems, Foster, CA). qPCR was performed with QuantStudio 3 Detection System (Thermo Fisher Scientific, Waltham, MA) in a 20 μl reaction mixture containing SYBR Green I (Thermo Fisher Scientific, Waltham, MA) in the following cycle condition: 95°C for 15 s, 60°C for 15 s, and 72°C for 25 s for 40 cycles in total. The level of expression of different genes was standardized with that of the housekeeping gene 18S rRNA and further analyzed using the $2^{-\Delta\Delta\text{CT}}$ method. All primers were synthesized by IDT (Skokie, IL) and their sequences are shown in Table S1.

2.11 | Statistics

ANOVA analysis was used for the experiments with multiple groups, a *p*-value of significance was set to be .05. The comparison of survival curves was analyzed using Log-rank (Mantel-Cox) ANOVA.

3 | RESULTS

3.1 | LipC6 in combination with α PD-1 Ab is unable to therapeutically suppress HCC growth

Given the capacity of LipC6 in inducing HCC apoptosis and preventing HCC-induced immune tolerance which was demonstrated by our previous research,¹⁷ we evaluated the therapeutic efficacy of α PD-1 Ab in combination with LipC6 in suppressing HCC with our murine model. HCC-bearing mice were randomly grouped to receive the following treatments: Control group with ghost

control and isotype control, LipC6 monotherapy, α PD-1 Ab monotherapy, and LipC6 in combination with α PD-1 Ab (Figure 1A). The time and dose courses of LipC6 and α PD-1 Ab have been optimized in our previous studies.^{16,17} Magnetic resonance imaging (MRI) was used to monitor tumor growth (Figure 1B). No significant difference in tumor size was detected by MRI in the mice across 4 groups on week 12 (Figure 1C). Macroscopic examination supports this finding, and no significant difference in tumor weights was detected in four groups of the mice with slightly decreased tumor weights found in LipC6-treated mice (Figure 1D,E). These results suggest that α PD-1 Ab in combination with LipC6 didn't induce a therapeutic effect in suppressing HCC. 5 weeks after the last treatment, we isolated the tumor-infiltrating leukocytes (TILs) in each mouse for flow cytometric assay. The results indicate that LipC6 monotherapy significantly increased CD8⁺ T cells and reduced FoxP3⁺ Tregs, no increased IFN- γ production in CD8⁺ T cells was detected in four groups of mice (Figure S2). Reversely α PD-1 Ab treatment promoted Treg generation (Figure S2C). These

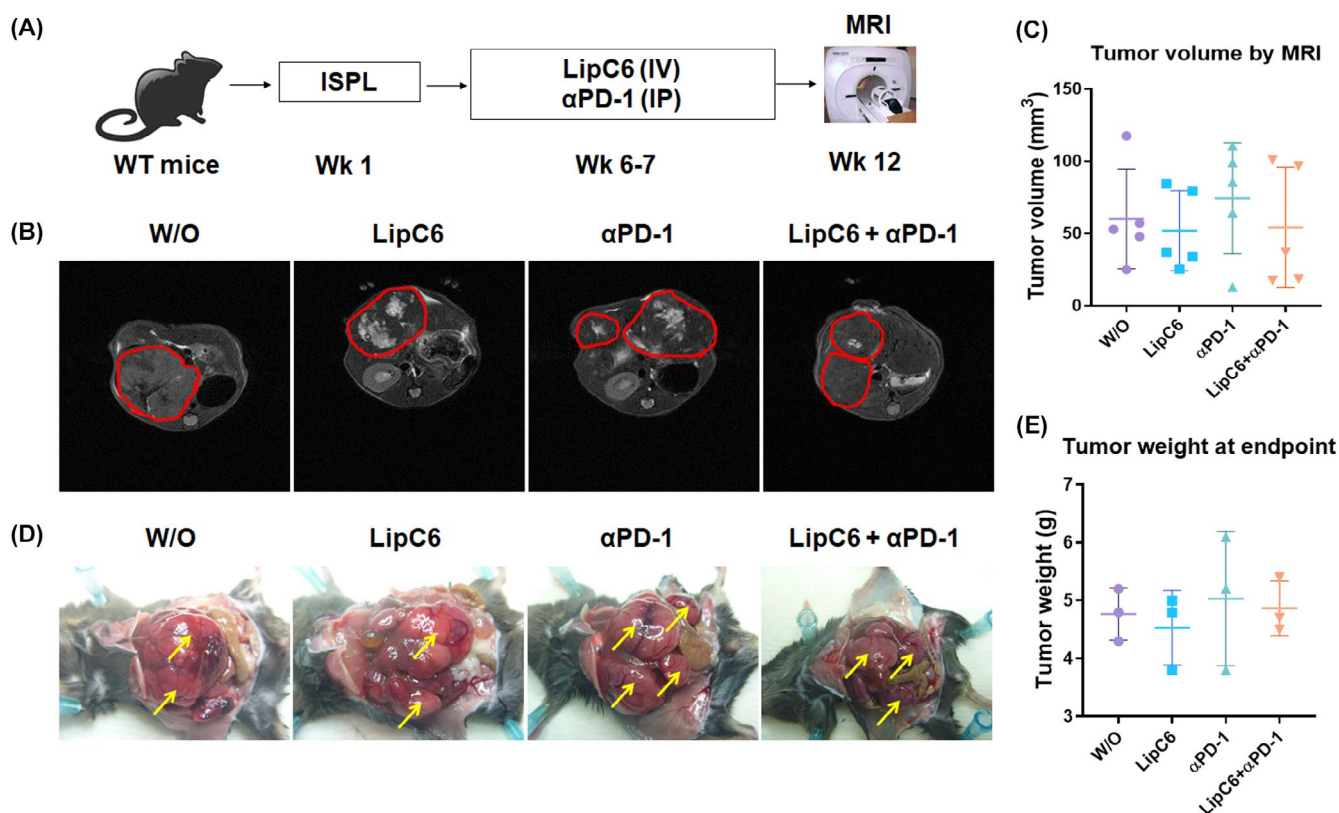


FIGURE 1 LipC6 in combination with α PD-1 Ab was unable to suppress HCC tumor growth. Tumor-bearing mice were randomly grouped to receive the treatments with LipC6, α PD-1 Ab, or both. Ghost (LipC6 vehicle control) and isotype Ab (α PD-1 Ab control) were used in control group (W/O). MRI was used to detect tumor growth in the mice three months after oncogenic hepatocyte inoculation. (A) Design of treatments with LipC6, α PD-1 Ab (α PD-1), and their combination. (B) Representative MRIs show tumor growth in response to the indicated treatments. Tumor nodules are outlined with red circles. (C) Accumulated tumor volumes in each mouse measured by MRI. The tumor volume was calculated by ImageJ. *n* = 5, error bars represent means \pm SD. (D) Macroscopic image of tumors. Yellow arrows point to the tumors. (E) Accumulated tumor weights in four groups of mice, *n* = 3, error bars represent means \pm SD

results suggest that α PD-1 Ab-driven increase of Tregs may contribute to the failure of α PD-1 Ab monotherapy and its combination with LipC6.

3.2 | LipC6 in combination with α CTLA4 Ab is efficacious in therapeutically suppressing HCC growth

Our previous studies have demonstrated that HCC-driven upregulation of PD-1 and CTLA4 in T cells contributes to tumor-induced immunotolerance.¹⁶ Thus, we examined whether LipC6 in combination with α CTLA4 Ab, rather than α PD-1 Ab, might be effective against HCC. As described above, the tumor-bearing mice were randomly grouped to receive the treatment with α CTLA4 Ab, LipC6, or both (Figure 2A). Five weeks post-treatment, MRI detected tumors significantly smaller in the mice with the combined treatment than control and each monotherapy (Figure 2B,C). The tumors in each mouse were also harvested to weigh, and tumor weight in the combined treatment group were significantly lighter than those in the other three groups of mice (Figure 2D,E). These data suggest the therapeutic efficacy of the combined treatment in suppressing HCC. IHC detected prominently increased expression of cleaved caspase 3 and cleaved PARP in tumors with the combined treatment, but not monotherapy (Figures 2F,G and S3), suggesting tumor apoptosis. Survival analysis indicates that LipC6 in combination with α CTLA4 Ab significantly extended the life span of tumor-bearing mice compared to the mice with or without monotherapy (Figure S4). Together, these results suggest that the LipC6 in combination with α CTLA4 Ab represents a new and powerful therapeutic approach in suppressing HCC.

3.3 | LipC6 in combination with α CTLA4 Ab induces activation of tumor-infiltrating effector CD8⁺ T cells

Next, we investigated whether the tumor suppression induced by the combinational treatment is linked to the activation of an anti-tumor immune response. For this reason, HCC-bearing mice were prepared and treated with LipC6, α CTLA4 Ab, or their combination as described in Figure 2. Five weeks post the last treatment, three mice in each group underwent liver perfusion to remove circulating cells, then tumors were harvested and used to isolate TILs. Flow cytometry detected a significantly increased frequency of CD8⁺ T cells in the gated CD3⁺ T cells in the mice receiving the combined treatment, but not either monotherapy. As shown in Figure 3A, ~35% of

tumor-resident CD8⁺ T cells were detected in the mice with the combined treatment, but only ~14%, ~21%, and ~24% of CD8⁺ T cells found in the control, α CTLA4 Ab-treated, and LipC6-treated mice. This increase was validated by IHC with anti-CD8a Ab which stained CD8⁺ T cells in the tumor sections in control and the treated mice (Figures 3B and S5). No significant alterations in the frequencies of tumor-resident NK cells (CD3⁻CD49b⁺NK1.1⁺) and NKT cells (CD3⁺NK1.1⁺) were detected across the four groups of mice (Figure S6). To examine whether the CD8⁺ T cell increase is accompanied by its activation, we detected the expression of CD69, an activation marker. As shown in Figure 3C, the frequency of the tumor-resident CD8⁺ T cells expressing CD69 in the mice with the combinational treatment (~36%) is significantly higher than that in control mice (~1.9%), α CTLA4 Ab-treated mice (~16%), and LipC6-treated mice (~5.1%). Furthermore, we evaluated the functional activation of effector CD8⁺ T cells in four groups of mice. For this purpose, the isolated TILs in each mouse were cultured with stimulation of TSA peptides for 5 h in the presence of Brefeldin A which blocks cytokine secretion, then the production of cytotoxic cytokines in cells was detected by flow cytometry. The results indicate that TSA epitope peptides caused a significant increase in the number of CD8⁺ T cells producing IFN- γ in the tumor-resident CD8⁺ T cells from mice with combined treatment relevant to control and either monotherapy (Figure 3D). While α CTLA4 Ab monotherapy caused the increased expression of CD69 in CD8⁺ T cells but didn't enhance IFN- γ production. Together, these data suggest that integration of LipC6 and α CTLA4 Ab activates tumor-resident CD8⁺ T cells phenotypically and functionally.

3.4 | LipC6 in combination with α CTLA4 Ab reduces KLF2 expression in tumor-resident CD8⁺ T cells

Transcriptional factors have been demonstrated to play an important role in manipulating tumor-induced T cell tolerance.²⁹ Our recent studies with single-cell RNA sequencing (scRNA-seq) have revealed that KLF2 is upregulated in tumor-resident CD8⁺ T cells in HCC-bearing mice compared to liver-resident CD8⁺ T cells in wild-type mice. Several previous studies show that KLF2 controls naïve Treg migration and maintains quiescence of naïve CD8⁺ T cells in association with peripheral tolerance.³⁰⁻³⁴ Thus, we examined whether KLF2 is a critical factor mediating LipC6-caused immune activation of CD8⁺ T cells. We isolated the TILs from the tumor-bearing mice with the indicated treatments and measured KLF2 expression in tumor-resident CD8⁺ T cells with flow cytometry. The results showed that the

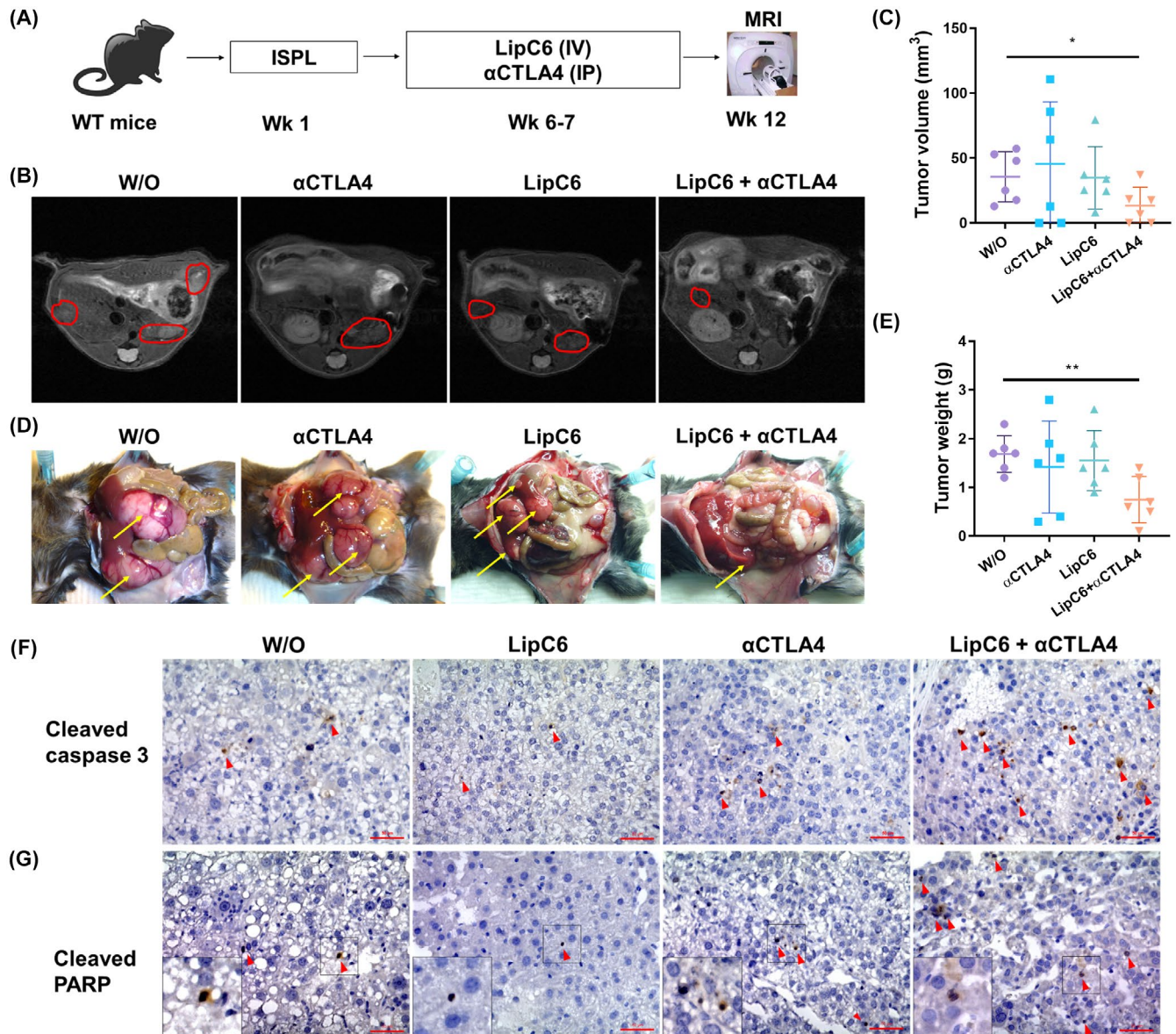


FIGURE 2 LipC6 in combination with αCTLA4 Ab suppressed HCC tumor progression. Tumor-bearing mice were randomly grouped to receive treatments with LipC6, αCTLA4 Ab, or both. Ghost (LipC6 vehicle control) and isotype Ab (αCTLA4 Ab control) were used in control group (W/O). MRI was used to detect tumor growth in the mice three months after oncogenic hepatocyte inoculation. (A) Design of treatment with LipC6, αCTLA4 Ab (αCTLA4), and their combination. (B) Representative MRI showing HCC tumor progression in response to indicated treatments. Tumor nodules are outlined by red circles. (C) Accumulated data of HCC tumor volume measured by MRI. The tumor volume was calculated by ImageJ. $n = 6$, $*p < .05$, error bars represent means \pm SD. (D) Macroscopic image of tumors. Yellow arrows point to the tumors. (E) Accumulated tumor weights in four groups of mice, $n = 6$, $**p < .01$, error bars represent means \pm SD. Representative images of IHC staining for cleaved caspase 3 (F) and cleaved PARP (G). Red arrows point to positive signals. Bars: 50 μ m

combined treatment, but not control or each monotherapy, significantly suppressed tumor-induced KLF2 up-regulation in tumor-resident CD8⁺ T cells to the levels in normal liver-resident CD8⁺ T cells (Figure 4A). Repeated experiments consistently generated similar results (Figure 4B), suggesting this finding is reliable. These results suggest that KLF2 may function as a transcriptional regulator to mediate CD8⁺ T cell activation induced by the combinational treatment of LipC6 and αCTLA4 Ab.

3.5 | In vitro treatment with LipC6 and αCTLA4 Ab reduces KLF2 expression in CD8⁺ T cells and Treg generation in normal splenocytes

To further identify cellular and molecular mediators underlying anti-tumor immune activation induced by LipC6 in combination with αCTLA4 Ab, we isolated RBC-depleted splenocytes in wild-type mice and treated these

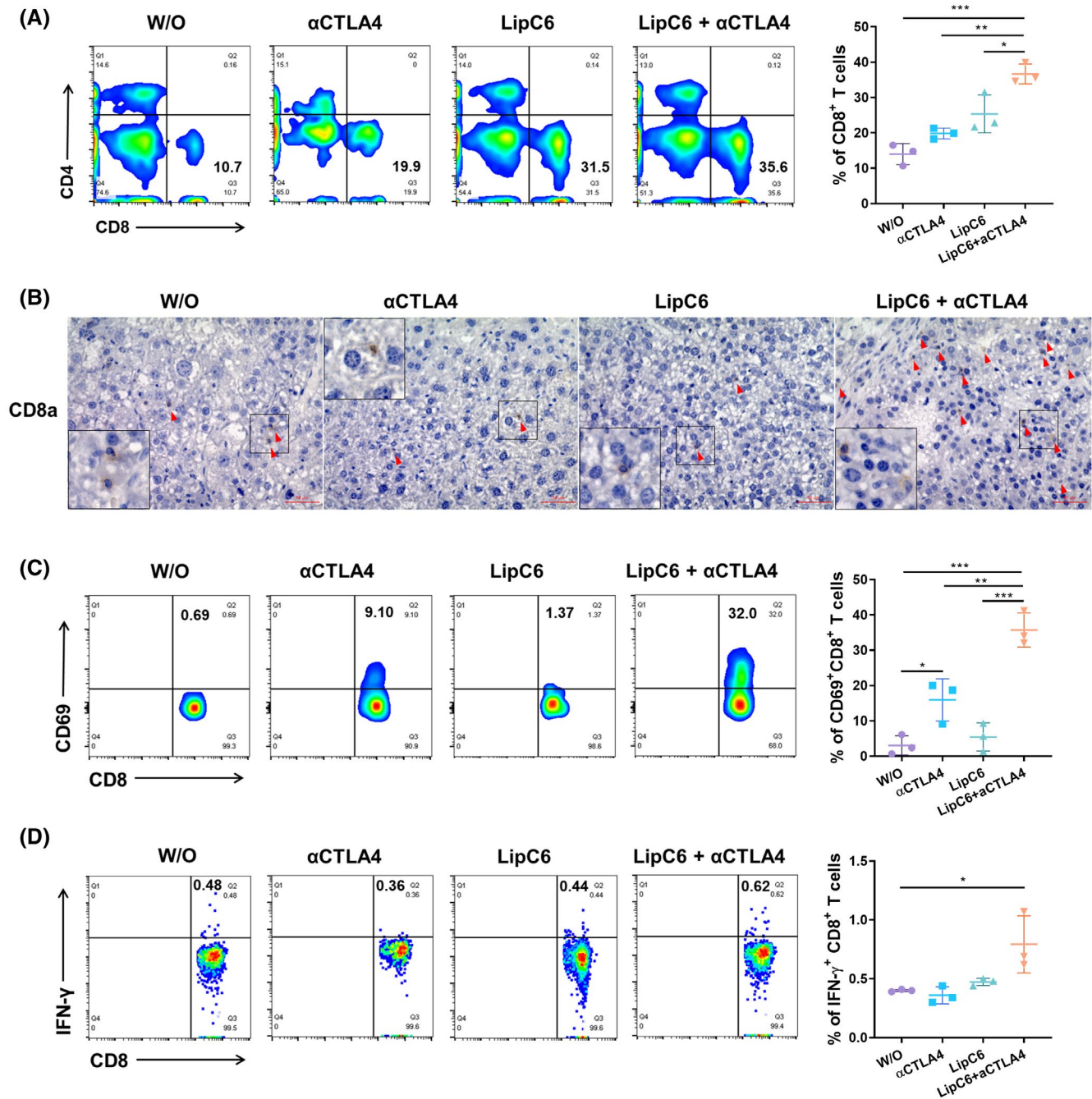


FIGURE 3 LipC6 in combination with αCTLA4 Ab activated intrahepatic effector CD8⁺ T cells. Tumor-bearing mice were randomly grouped to receive the indicated treatments as shown in Figure 2. Five weeks post-treatment, the mice were sacrificed, and TILs were isolated for flow cytometry. (A) Representative and accumulated frequency of tumor-infiltrating CD8⁺ T cells in four groups of mice. $n = 3$, * $p < .05$, ** $p < .01$, *** $p < .001$, error bars represent means \pm SD. (B) Representative images of IHC staining for CD8⁺ T cells. Red arrows point to the positive staining cells, bars: 50 μ m. (C) Representative and accumulated frequency of tumor-infiltrating CD69⁺CD8⁺ T cells in four groups of mice. $n = 3$, * $p < .05$, ** $p < .01$, *** $p < .001$, error bars represent means \pm SD. (D) Representative and accumulated frequency of IFN- γ -producing CD8⁺ T cell in the TILs isolated from four groups of mice in response to TSA stimulation. The cultured TILs were stimulated with large T antigen (TAg) epitopes I and IV in the presence of Brefeldin A. Five hours post-stimulation, IFN- γ -producing CD8⁺ T cells were evaluated by flow cytometry. $n = 3$, * $p < .05$, error bars represent means \pm SD

cells with LipC6, αCTLA4 Ab, or their combination in the presence of anti-CD3 and anti-CD28 Abs for 24 h. Flow cytometry detected the significantly increased frequency of CD8⁺ T cells in splenocytes receiving αCTLA4 Ab (~11%),

LipC6 (~27%), and the combined treatment (~29%) in comparison to that in the control (~7%) (Figure 5A); the expression of CTLA4 in CD8⁺ T cells was suppressed by LipC6 treatment (Figure 5B); the reduced frequency of

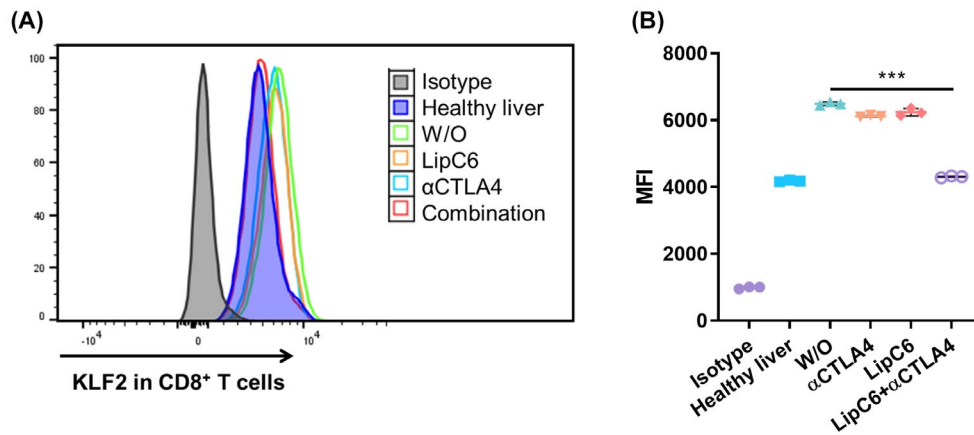


FIGURE 4 LipC6 in combination with α CTLA4 Ab suppressed KLF2 expression in tumor-infiltrating CD8⁺ T cells. Tumor-bearing mice were randomly grouped to receive the indicated treatments as shown in Figure 2. Five weeks after the last treatment, the TILs were isolated. KLF2 expression in CD8⁺ T cells was detected by flow cytometry. (A) Representative histogram showing KLF2 expression in tumor-infiltrating CD8⁺ T cells in four groups of mice. Liver-infiltrating CD8⁺ T cells from normal mice were used for control. (B) Accumulated data of KLF2 expression in tumor-infiltrating CD8⁺ T cells in four groups of mice. Liver-infiltrating CD8⁺ T cells from normal mice were used for control. $n = 3$, *** $p < .001$, error bars represent means \pm SD

CD4⁺CD25⁺FoxP3⁺ Treg in the cells with LipC6 monotherapy or combination with α CTLA4 Ab (Figure 5C). In accompany with these effects, we also detected the decreased expression of KLF2 in T cells treated with LipC6 or its combination with α CTLA4 Ab (Figure 5D). Together, these results suggest the correlation of LipC6-induced immune activation with Treg suppression and reduced expression of CTLA4 and KLF2.

3.6 | KLF2 mediates the effect of LipC6 in promoting CD8⁺ T cell proliferation and decreasing Treg production

To define whether KLF2 as a factor mediates the effect of LipC6 on CD8⁺ T cells and Tregs, we purified pan T cells in splenocytes from wild-type mice and cultured the cells in the presence of anti-CD3 and anti-CD28 Abs. We treated these cells with Klf2 siRNA (Figure S7), LipC6, or their combination. The combined treatment was conducted by siRNA transfection, followed by LipC6 treatment on the second day. 24 h later, the cells were harvested to detect the frequency of CD8⁺ T cells and Tregs with flow cytometry. The significantly increased frequencies of CD8⁺ T cells were found in the splenocytes treated with LipC6 (~23%), siRNA transfection (~22%), or the combination (~26%) relevant to ~16% CD8⁺ T cells in the control cells treated with ghost (Figure 6A); and the significantly reduced frequencies of CD4⁺CD25⁺FoxP3⁺ Tregs were also detected in the splenocytes treated with LipC6 (~0.14%), siRNA transfection (~0.59%), or the combination (~0.35%) relevant to ~0.9% CD4⁺CD25⁺FoxP3⁺ Tregs in the control

cells treated with ghost (Figure 6B). We found that the combined treatment did not induce an additional effect on CD8⁺ T cells and Tregs in the splenocytes compared to each monotherapy. These results indicate that KLF2 may function as a factor contributing to LipC6's effect in promoting CD8⁺ T cells and suppressing Tregs.

3.7 | Molecular events in association with T cell activation induced by α CTLA4 Ab or/and LipC6

To reveal molecular events associated with immune activation induced by LipC6 or/and α CTLA4 Ab, we purified pan T cells from splenocytes in wild-type mice and treated them with LipC6, α CTLA4 Ab, or their combination in the presence of anti-CD3 & anti-CD28 Abs. 24 h later, the cells were harvested and used for qPCR. The results showed that LipC6, but not α CTLA4 Ab, significantly reduced the expression of Klf2, Foxp3, and Ctla4. In addition, both monotherapies and combination treatment did not influence the expression of PD-1 gene (Pdcd1) in T cells (Figure 7A–D). We also detected the increased gene expression of Granzyme B (Gzmb) (Figure 7E) and TNF- α (Tnf) (Figure 7F) in the cells treated with either LipC6 or its combination with α CTLA4 Ab. However, the increased expression of IFN- γ (Ifng) was only detected in the cells with the combined treatment, but not monotherapies (Figure 7G). These results suggest that LipC6 selectively modulates the expression of immune checkpoints and the production of functional cytokines.

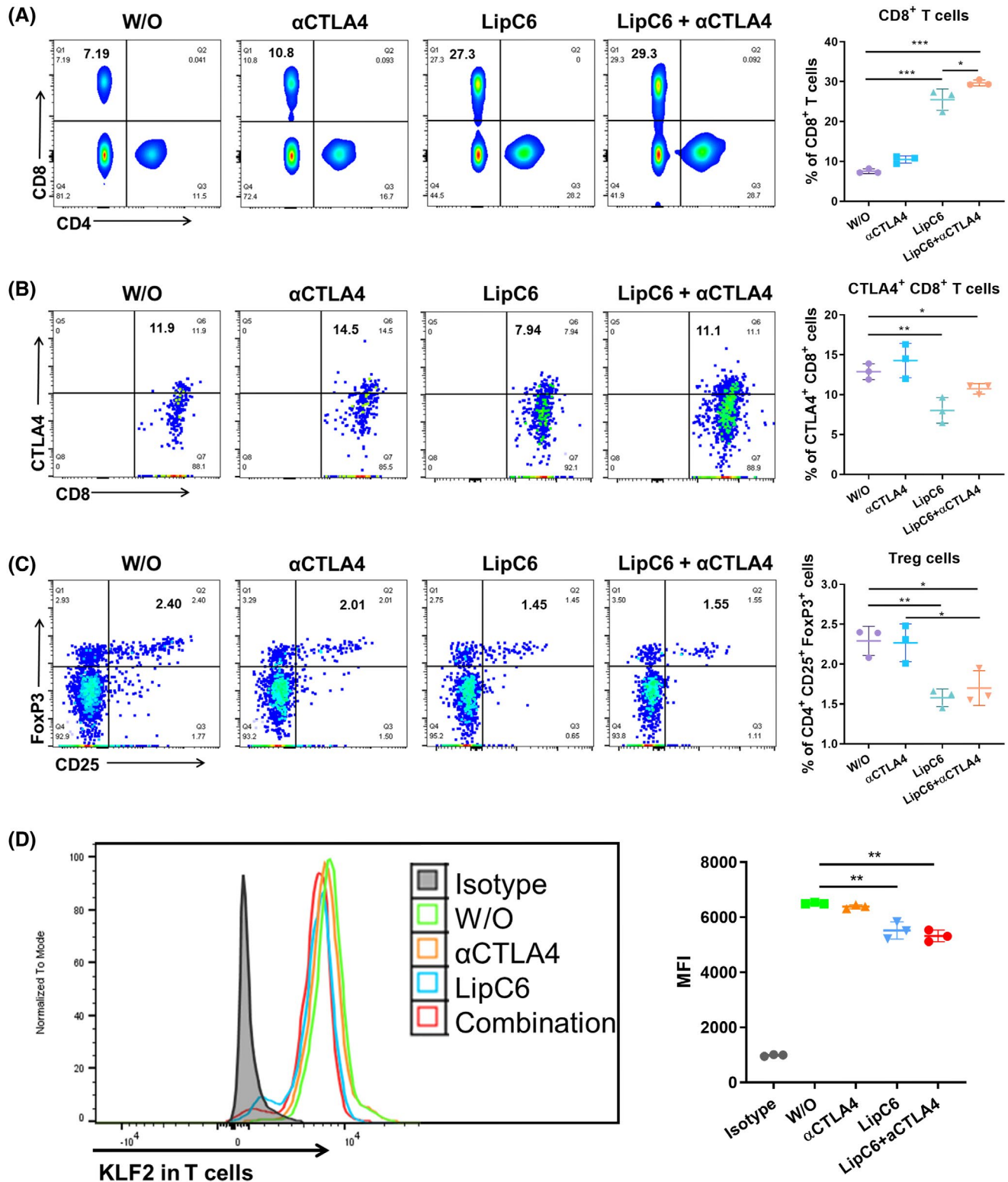


FIGURE 5 LipC6 reduced the generation of FoxP3⁺ Tregs and the expression of CTLA4 and KLF2 in CD8⁺ T cells in vitro. Naive C57BL/6 mice were used to prepare RBC-depleted splenocytes. These cells received the indicated treatments with LipC6, α CTLA4, or both in the presence of anti-CD3 & anti-CD28 Abs for 24 h for flow cytometric assay. Ghost (LipC6 vehicle control) and isotype Ab (α CTLA4 Ab control) were used in control group (W/O). (A) Representative flow cytometry and accumulated data showing the frequency of CD8⁺CD3⁺ T cells in the splenocytes in response to the different treatments. $n = 3$, * $p < .05$, ** $p < .01$, *** $p < .001$, error bars represent means \pm SD. (B) Representative flow cytometry and accumulated data showing frequency of CTLA4⁺CD8⁺ T cells in the splenocytes in response to the different treatments. $n = 3$, * $p < .05$, ** $p < .01$, error bars represent means \pm SD. (C) Representative flow cytometry and accumulated data showing the frequency of CD4⁺CD25⁺ FoxP3⁺ Treg cells in the splenocytes in response to the different treatments. $n = 3$, * $p < .05$, ** $p < .01$, error bars represent means \pm SD. (D) Representative flow cytometry and accumulated data showing KLF2 expression in CD3⁺ T cells in the splenocytes in response to the different treatments. $n = 3$, ** $p < .01$, error bars represent means \pm SD

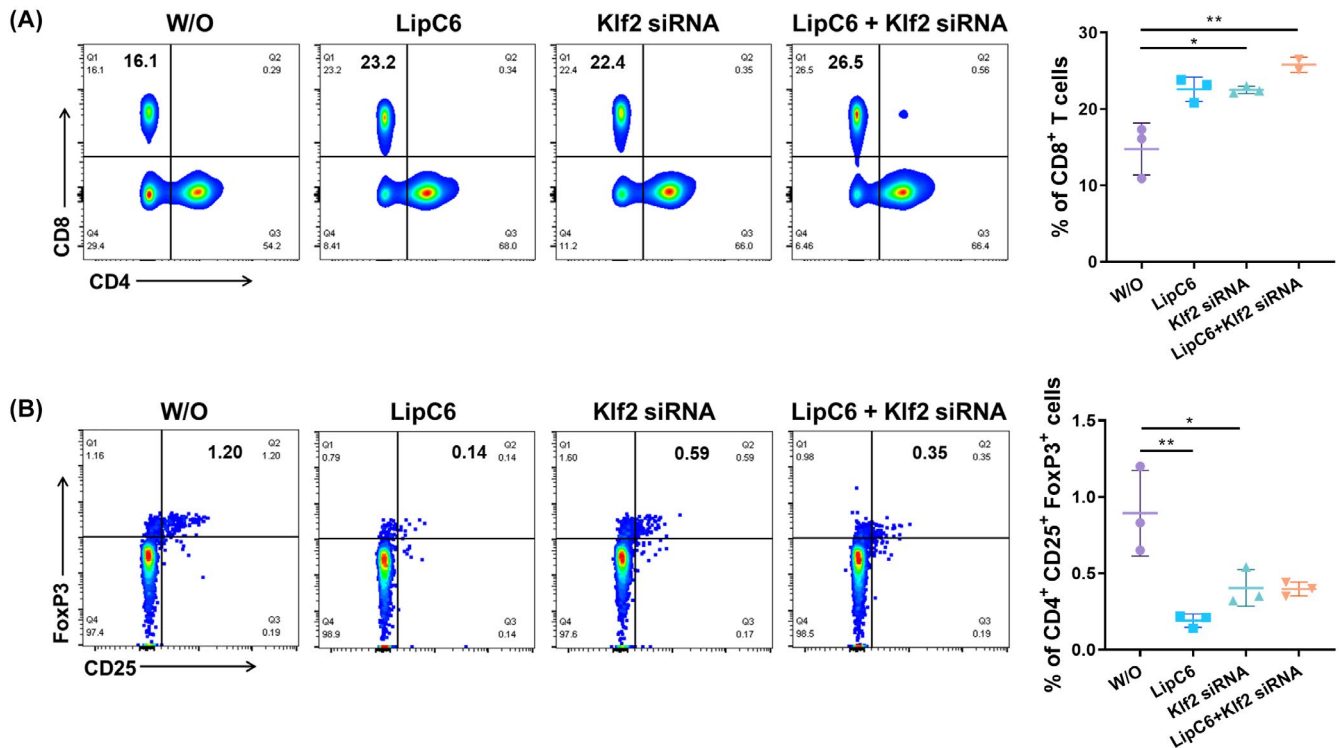


FIGURE 6 siRNA-mediated KLF2 knockdown compensates for LipC6-induced increase in the frequency of CD8⁺ T cells and decrease in the frequency of Tregs. The pan T cells purified from splenocytes in wild-type mice via negative selection beads. These cells respectively received LipC6 treatment, Klf2 siRNA transfection, or both in the presence of anti-CD3 & anti-CD28 Abs. Ghost (LipC6 vehicle control) and scrambled siRNA (Klf2 siRNA control) were used in control group (W/O). 24 h, the cells were harvested for flow cytometry. (A) Representative frequency and accumulated data of CD8⁺CD3⁺ T cells in the splenocytes with the indicated treatments. *n* = 3, **p* < .05, ***p* < .01, error bars represent means ± SD. (B) Representative frequency and accumulated data of CD4⁺CD25⁺FoxP3⁺ Tregs in the splenocytes with the indicated treatments. *n* = 3, **p* < .05, ***p* < .01, error bars represent means ± SD

4 | DISCUSSION

We have developed a new therapeutic approach for HCC treatment by integrating our patented LipC6 with αCTLA4 Ab. The results indicate that LipC6 in combination with αCTLA4 Ab significantly suppresses orthotopic HCC tumor growth. This effect is implicated in the activation of anti-tumor immunity induced by LipC6 via suppressing Treg and CTLA4. The non-influenced PD-1 expression by LipC6 and the increased Tregs induction by αPD-1 Ab may explain why LipC6 in combination with αCTLA4 Ab, but not αPD-1 Ab, offers a therapeutic effect in suppressing HCC.

We developed a new ICB-integrated therapeutic approach by combining αCTLA4 Ab with LipC6 which satisfies the unmet needs in HCC treatment, highlighting its clinical value. HCC is the third-highest cause of cancer-related death without effective therapies.³⁻⁵ Sorafenib, a receptor tyrosine kinase inhibitor, is the first approved systemic chemotherapy for advanced HCC, but only increases patient median overall survival from 7.9 to 10.7 months.¹² Immune checkpoint therapy (ICT) can generate an unprecedented and durable clinical

response. Ab-mediated blockade of CTLA-4, PD-1, or its ligand PD-L1 have been approved by the FDA to treat several types of cancer.³⁵⁻³⁸ Encouraged by the strength of mid-stage clinical trial data, αPD1 Ab was awarded an accelerated approval in 2017 for second-line treatment of HCC. However, the follow-up larger multi-center phase III study failed to demonstrate the efficacy of αPD1-Ab in improving patient survival over controls.^{15,39} Thus, Bristol Myers Squibb announced that αPD1 Ab as a single agent for the treatment of HCC patients previously treated with sorafenib was withdrawn from the US market on July 26, 2021. While the combination of αPD-L1 Ab and αVEGF-A Ab was approved in May 2020 to use in patients with unresectable HCC, the median progression-free survival (PFS) is only 6.8 months versus 4.3 months with sorafenib treatment. Thus, there is an urgent need to dissect the underlying mechanisms and identify new critical targets for developing novel therapeutic approaches to improve ICT against HCC. Phase I clinical trial of the patented LipC6 has been recently completed (NCT#02834611).⁴⁰ Our recent studies led to the new findings that LipC6 has the capacity to break HCC-induced immune tolerance.¹⁷ Of particular

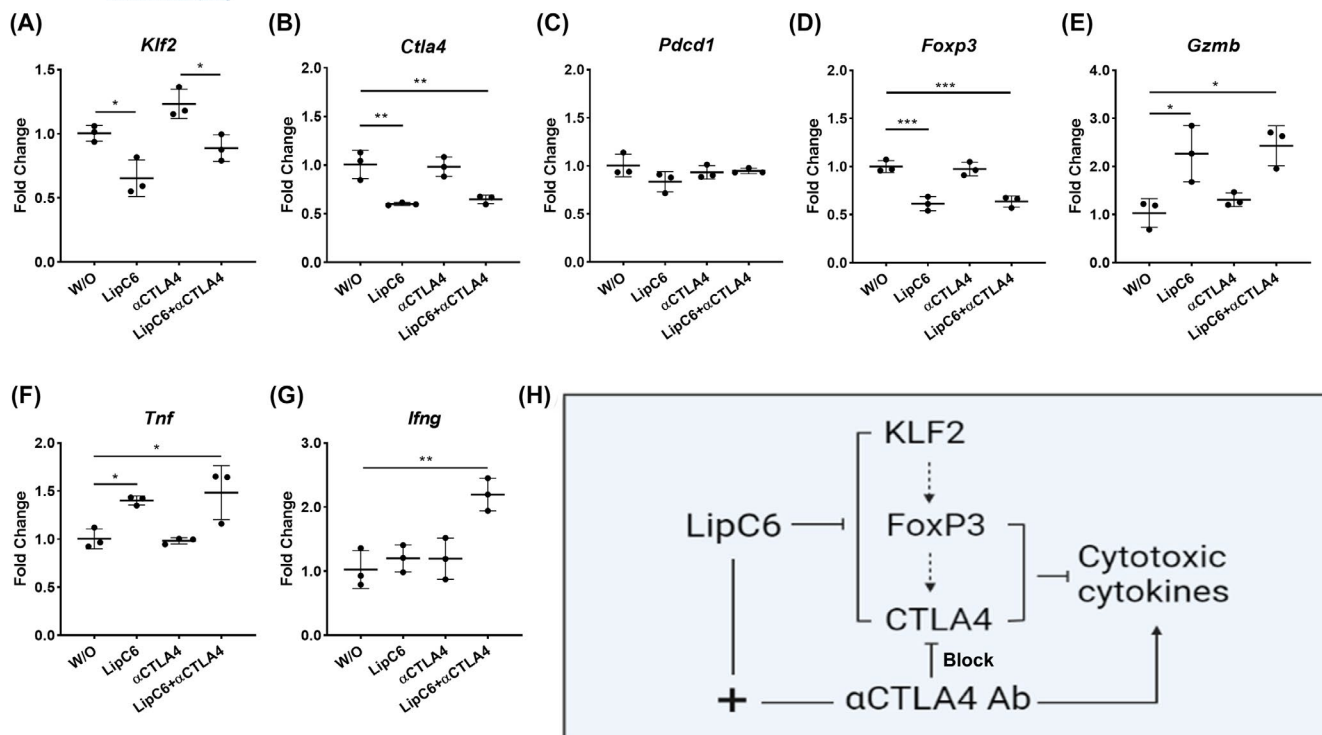


FIGURE 7 Molecular actions of LipC6, α CTLA4 Ab, or their combination on T cells. Pan T cells purified from splenocytes in wild-type mice with negative selection beads. These cells respectively received the treatments of LipC6, α CTLA4 Ab or both in the presence of anti-CD3 & anti-CD28 Abs. Ghost (LipC6 vehicle control) and isotype Ab (α CTLA4 Ab control) were used in control group (W/O). 24 h later, the cells were harvested to extract total RNAs for detecting the expression of the indicated genes by qPCR. The expression level of the indicated genes was normalized to housekeeping genes. The fold changes of each gene were shown for *Klf2* (A), *Ctla4* (B), *Pdccl1* (C), *Foxp3* (D), *Gzmb* (E), *Tnf* (F), and *Ifng* (G). * $p < .05$, ** $p < .01$, *** $p < .001$. $n = 3$, Error bars represent means \pm SD. (G) Schematic diagram depicting the signal pathways mediating combinatorial function of LipC6 and α CTLA4 Ab

importance, we have now demonstrated that LipC6 treatment significantly improves α CTLA-4 Ab's therapeutic suppression on HCC. Also, α CTLA-4 Ab has been used in human patients. Thus, LipC6 in combination with α CTLA-4 Ab can be quickly translated into the clinical application for HCC treatment. Hage et al. reported that combined treatment with α PD1 Ab and α CTLA4 Ab generated the response in the transplanted Hep-55 model, but not in the transgenic iAST model, suggesting combined blockade of PD1 and CTLA4 has a selective effect in suppressing tumor growth.⁴¹ We are going to further test the therapeutic efficacy of LipC6 in combination with both α CTLA4 and α PD1 Abs in HCC treatment.

LipC6 in combination with α CTLA4 Ab, but not α PD-1 Ab, therapeutically suppresses tumor growth (Figures 1 and 2). This may be involved in the effect of this combinational treatment on PD-1 expression and Treg induction. In the present studies, we have found that LipC6 suppresses CTLA4 and Treg. Our previous studies demonstrated that LipC6 significantly modulates tumor-associated macrophages (TAMs) by preventing its polarization to M2 phenotype, resulting in TSA immune

activation.¹⁷ Tumor-resident Tregs highly express CTLA4. Therefore, it is likely that LipC6-primed TAMs destroy α CTLA-4 Ab-opsonized Tregs via Ab dependent cellular phagocytosis (ADCP) as it was found in other studies.^{42,43} In contrast, Hiroyoshi Nishikawa group found PD-1 blockade induces increased tumor-infiltrating Tregs^{44,45} which may compromise LipC6-caused immune activation. This assumption is supported by our finding in the current studies in which LipC6 in combination with α PD-1 Ab failed to promote CD8⁺ T cell increase, advance its IFN- γ production, and suppress Treg induction (Figure S2).

Different from our previous finding,¹⁷ the current studies did not show that LipC6 monotherapy significantly suppresses HCC growth. This may be associated with the difference of previous and current studies in tumor models and tumor sizes when receiving the treatment. In the present study, we established tumor-bearing mice via ISPL injection of oncogenic hepatocytes without inducing liver fibrosis with CCl₄. Also, we treated the mice bearing the tumors much less than 50 mm³, relevant to more than 150 mm³ in our previous studies. And, the mice were euthanized 5 weeks after the last treatment. At this time point, the tumor size in

each mouse across four groups is still very small, suggesting early-stage tumors. These factors can explain why LipC6 monotherapy did not show the therapeutic effect on HCC. We are now making the murine model with liver fibrosis and will treat the tumor-bearing mice after tumors are beyond 150 mm³. The results will be reported in the future.

It is novel to find that LipC6 directly activates T cells independent on other cells including NK and NKT cells (Figure S6). We initially discovered that LipC6 induces activation of TSA CD8⁺ T cells which is associated with modulation of TAMs into M1 phenotype.¹⁷ Here, we isolated pan T cells in splenocytes by negative selection with magnetic beads, which removes all other cells, including macrophages, NK, and NKT cells. Treatment of pan T cells with LipC6 markedly promotes anti-CD3 and anti-CD28 Abs-induced proliferation of CD8⁺ T cells (Figure 5A), associated with its suppression on CTLA4 expression (Figure 5B) and Tregs generation (Figure 5C). These results suggest that LipC6 directly activates T cells independent of its effect on macrophages. Yet, our *in vitro* and *in vivo* studies demonstrate that LipC6 monotherapy, without combination with α CTLA4 Ab, could enhance CD8⁺ T cell proliferation (Figures 3A and 5A) but could not functionally activate CD8⁺ T cells to produce INF γ (Figure 3C). Taken together, these results suggest that a combinatorial therapeutic approach with LipC6 and α CTLA4 Ab could significantly prime immune activation and generate an anti-tumor effect, offering a better chance of treating HCC. A recent randomized combinatorial clinical trial demonstrates that nivolumab (α PD-1 Ab) plus ipilimumab (α CTLA4 Ab) shows a manageable safety profile, a promising objective response rate, and a durable response in human patients with advanced HCC who were previously treated with sorafenib.³⁷ This strategy received accelerated approval in the US based on these results.⁴⁶ Our team has also generated data to support other combinatorial therapeutic approaches for HCC, including LipC6 plus TSA CD8⁺ T cells,¹⁷ Sunitinib plus α PD-1 Ab,¹⁶ Sunitinib plus Radiofrequency ablation (RFA),²¹ and laser ablation plus immune-activator *N*-dihydro-galacto-chitosan (GC).²⁸ Together, these pre-clinical and clinical studies indicate that combinatorial therapeutic strategies represent a promising approach in HCC treatment.

Our studies describe the molecular events underlying LipC6-induced immune activation, including regulation of KLF2, FoxP3, and CTLA4. Our *in vivo* and *in vitro* studies show that LipC6 significantly suppresses KLF2, FoxP3, and CTLA4 (Figures 4, 5B–D, 6B, and 7). Both CTLA4 and FoxP3 pathways represent complementary and largely overlapping mechanisms that are essential for the control of immune homeostasis and immune

tolerance.⁴⁷ KLF2 is linked to regulation of immune tolerance in different ways, such as (1) regulating S1PR1⁴⁸ and chemokine receptors (CXCR3 and CXCR5) to suppress inflammatory cell adhesion in endothelial cells⁴⁹ and effector T cell function. S1PR1 is a receptor for sphingosine-1-phosphate that is antagonized by ceramide. (2) down-regulating c-Myc pathway to maintain T cell quiescence.³⁴ (3) functioning as a transcription factor to upregulate FoxP3 expression by binding to its promoter to modulate the development of inducible Treg.³⁰ FoxP3 can bind to the CTLA4 promoter to increase its histone acetylation at this region, and the resultant modification of chromatin structure facilitates CTLA4 transcription.⁵⁰ These results imply that KLF2, FoxP3, and CTLA4 as molecular bases mediate LipC6-induced immune activation. More effort is required to test this hypothesis and elucidate the underlying mechanisms.

In conclusion, we have developed and demonstrated LipC6/ α CTLA4 Ab as a promising novel therapeutic strategy to suppress HCC. LipC6 and α CTLA4 Ab synergize to effectively activate anti-HCC immune response which is associated with the repression of Treg and suppressing KLF2, FoxP3, and CTLA4.

ACKNOWLEDGMENTS

The authors thank Dr. Lixin Ma in VA-BIC in the Harry S. Truman Memorial Veterans' Hospital for the assistance in conducting MRI to monitor tumor growth.

DISCLOSURES

Penn State Research Foundation has licensed LipC6 technology to Keystone Nano Inc (PA) and Mark Kester is CTO and cofounder of Keystone Nano.

AUTHOR CONTRIBUTIONS

Kevin F. Staveley-O'Carroll, Mark Kester and Guangfu Li conceived and designed the research; Xiaoqiang Qi, Feng Wu and Sung Hoon Kim performed the research and acquired the data; Xiaoqiang Qi, Jussuf T. Kaifi, Eric T. Kimchi analyzed and interpreted the data; Helena Snyder, Anuradha Illendula, Todd Fox and Mark Kester contributed the new reagents; All authors were involved in drafting and revising the manuscript.

ETHICS APPROVAL

All mice used in these studies were housed, managed, and cared for per the Guide for the Care and Use of Laboratory Animals (National Research Council, 2011) and were conformed to the Animal Research: Reporting of In Vivo Experiments (ARRIVE) guidelines. And all animal experiments were approved by the Institutional Animal Care and Use Committee (IACUC) of the University of Missouri (Columbia, MO).

STATEMENT

All authors had access to the study data and had reviewed and approved the final manuscript.

DATA AVAILABILITY STATEMENT

Data are available upon reasonable request. The data sets used and/or analyzed during the current study are available from the corresponding author upon reasonable request.

ORCID

Guangfu Li  <https://orcid.org/0000-0002-9817-568X>

REFERENCES

- Llovet JM, Zucman-Rossi J, Pikarsky E, et al. Hepatocellular carcinoma. *Nat Rev Dis Primers*. 2016;2:16018. doi:10.1038/nrdp.2016.18
- Llovet JM, Kelley RK, Villanueva A, et al. Hepatocellular carcinoma. *Nat Rev Dis Primers*. 2021;7(1):6. doi:10.1038/s41572-020-00240-3
- O'Conner S, Ward JW, Watson M, Momin B, Richardson LC. Hepatocellular carcinoma—United States, 2001-2006. *MMWR Morb Mortal Wkly Rep*. 2010;59(17):517-520.
- Petrack JL, Kelly SP, Altekruse SF, McGlynn KA, Rosenberg PS. Future of hepatocellular carcinoma incidence in the United States forecast through 2030. *J Clin Oncol*. 2016;34(15):1787-1794. doi:10.1200/JCO.2015.64.7412
- Colombo M, Maisonneuve P. Controlling liver cancer mortality on a global scale: still a long way to go. *J Hepatol*. 2017;67(2):216-217. doi:10.1016/j.jhep.2017.05.004
- Clavien PA, Lesurtel M, Bossuyt PM, et al.; Group OLTfHC. Recommendations for liver transplantation for hepatocellular carcinoma: an international consensus conference report. *Lancet Oncol*. 2012;13(1):e11-e22. doi:10.1016/S1470-2045(11)70175-9
- Vitale A, Peck-Radosavljevic M, Giannini EG, et al. Personalized treatment of patients with very early hepatocellular carcinoma. *J Hepatol*. 2017;66(2):412-423. doi:10.1016/j.jhep.2016.09.012
- Cucchetti A, Cescon M, Pinna AD. Portal hypertension and the outcome of surgery for hepatocellular carcinoma in compensated cirrhosis: A systematic review and meta-analysis. More doubts than clarity. *Hepatology*. 2015;62(3):976-977. doi:10.1002/hep.27702
- Vitale A, Cucchetti A, Qiao GL, et al. Is resectable hepatocellular carcinoma a contraindication to liver transplantation? A novel decision model based on “number of patients needed to transplant” as measure of transplant benefit. *J Hepatol*. 2014;60(6):1165-1171. doi:10.1016/j.jhep.2014.01.022
- Mancuso A. Hepatocellular carcinoma in thalassaemia—emerging issues and challenges for liver transplant. *Aliment Pharmacol Ther*. 2014;40(11-12):1368-1369. doi:10.1111/apt.12989
- Kim HD, Shim JH, Kim GA, et al. Optimal methods for measuring eligibility for liver transplant in hepatocellular carcinoma patients undergoing transarterial chemoembolization. *J Hepatol*. 2015;62(5):1076-1084. doi:10.1016/j.jhep.2014.12.013
- Llovet JM, Di Bisceglie AM, Bruix J, et al. Panel of experts in HCCDCT. Design and endpoints of clinical trials in hepatocellular carcinoma. *J Natl Cancer Inst*. 2008;100(10):698-711. doi:10.1093/jnci/djn134
- Andrews MC, Wargo JA. Cancer evolution during immunotherapy. *Cell*. 2017;171(4):740-742. doi:10.1016/j.cell.2017.10.027
- Havel JJ, Chowell D, Chan TA. The evolving landscape of biomarkers for checkpoint inhibitor immunotherapy. *Nat Rev Cancer*. 2019;19(3):133-150. doi:10.1038/s41568-019-0116-x
- Arthur B. Checkpoint Immunotherapy Approved for Patients with Stomach, Gastroesophageal, and Liver Cancer, September 25, 2017.
- Li G, Liu D, Cooper TK, et al. Successful chemoimmunotherapy against hepatocellular cancer in a novel murine model. *J Hepatol*. 2017;66(1):75-85. doi:10.1016/j.jhep.2016.07.044
- Li G, Liu D, Kimchi ET, et al. Nanoliposome C6-ceramide increases the anti-tumor immune response and slows growth of liver tumors in mice. *Gastroenterology*. 2018;154(4):1024-1036.e9. doi:10.1053/j.gastro.2017.10.050
- Avella DM, Li G, Schell TD, et al. Regression of established hepatocellular carcinoma is induced by chemoimmunotherapy in an orthotopic murine model. *Hepatology*. 2012;55(1):141-152. doi:10.1002/hep.24652
- Mittal S, El-Serag HB. Epidemiology of hepatocellular carcinoma. *J Clin Gastroenterol*. 2013;47(Suppl 1):S2-S6. doi:10.1097/MCG.0b013e3182872f29
- Qi X, Li G, Liu D, et al. Development of a radiofrequency ablation platform in a clinically relevant murine model of hepatocellular cancer. *Cancer Biol Ther*. 2015;16(12):1812-1819. doi:10.1080/15384047.2015.1095412
- Qi X, Yang M, Ma L, et al. Synergizing sunitinib and radiofrequency ablation to treat hepatocellular cancer by triggering the antitumor immune response. *J Immunother Cancer*. 2020;8(2):e001038. doi:10.1136/jitc-2020-001038
- Tagaram HR, Divittore NA, Barth BM, et al. Nanoliposomal ceramide prevents in vivo growth of hepatocellular carcinoma. *Gut*. 2011;60(5):695-701. doi:10.1136/gut.2010.216671
- Liu JW, Beckman BS, Foroozesh M. A review of ceramide analogs as potential anticancer agents. *Future Med Chem*. 2013;5(12):1405-1421. doi:10.4155/fmc.13.107
- Morad SA, Cabot MC. Ceramide-orchestrated signalling in cancer cells. *Nat Rev Cancer*. 2013;13(1):51-65. doi:10.1038/nrc3398
- Kester M, Bassler J, Fox TE, Carter CJ, Davidson JA, Parette MR. Preclinical development of a C6-ceramide NanoLiposome, a novel sphingolipid therapeutic. *Biol Chem*. 2015;396(6-7):737-747.
- Liu X, Ryland L, Yang J, et al. Targeting of survivin by nanoliposomal ceramide induces complete remission in a rat model of NK-LGL leukemia. *Blood*. 2010;116(20):4192-4201. doi:10.1182/blood-2010-02-271080
- Held WA, Mullins JJ, Kuhn NJ, Gallagher JF, Gu GD, Gross KW. T antigen expression and tumorigenesis in transgenic mice containing a mouse major urinary protein/SV40 T antigen hybrid gene. *EMBO J*. 1989;8(1):183-191.
- Qi X, Lam SS, Liu D, et al. Development of inCVAX, in situ cancer vaccine, and its immune response in mice with hepatocellular cancer. *J Clin Cell Immunol*. 2016;7(4):438. doi:10.4172/2155-9899.1000438

29. Nurieva R, Wang J, Sahoo A. T-cell tolerance in cancer. *Immunotherapy*. 2013;5(5):513-531. doi:10.2217/imt.13.33
30. Pabbisetty SK, Rabacal W, Maseda D, et al. KLF2 is a rate-limiting transcription factor that can be targeted to enhance regulatory T-cell production. *Proc Natl Acad Sci U S A*. 2014;111(26):9579-9584. doi:10.1073/pnas.1323493111
31. Preston GC, Feijoo-Carnero C, Schurch N, Cowling VH, Cantrell DA. The impact of KLF2 modulation on the transcriptional program and function of CD8 T cells. *PLoS One*. 2013;8(10):e77537. doi:10.1371/journal.pone.0077537
32. Kuo CT, Veselits ML, Leiden JM. LKLF: a transcriptional regulator of single-positive T cell quiescence and survival. *Science*. 1997;277(5334):1986-1990. doi:10.1126/science.277.5334.1986
33. Sebзда E, Zou Z, Lee JS, Wang T, Kahn ML. Transcription factor KLF2 regulates the migration of naive T cells by restricting chemokine receptor expression patterns. *Nat Immunol*. 2008;9(3):292-300. doi:10.1038/ni1565
34. Buckley AF, Kuo CT, Leiden JM. Transcription factor LKLF is sufficient to program T cell quiescence via a c-Myc-dependent pathway. *Nat Immunol*. 2001;2(8):698-704. doi:10.1038/90633
35. Gao J, Ward JF, Pettaway CA, et al. VISTA is an inhibitory immune checkpoint that is increased after ipilimumab therapy in patients with prostate cancer. *Nat Med*. 2017;23(5):551-555. doi:10.1038/nm.4308
36. Hahn AW, Gill DM, Pal SK, Agarwal N. The future of immune checkpoint cancer therapy after PD-1 and CTLA-4. *Immunotherapy*. 2017;9(8):681-692. doi:10.2217/imt-2017-0024
37. Postow MA, Callahan MK, Wolchok JD. Immune checkpoint blockade in cancer therapy. *J Clin Oncol*. 2015;33(17):1974-1982. doi:10.1200/JCO.2014.59.4358
38. Remon J, Besse B. Immune checkpoint inhibitors in first-line therapy of advanced non-small cell lung cancer. *Curr Opin Oncol*. 2017;29(2):97-104. doi:10.1097/CCO.0000000000000351
39. El-Khoueiry AB, Sangro B, Yau T, et al. Nivolumab in patients with advanced hepatocellular carcinoma (CheckMate 040): an open-label, non-comparative, phase 1/2 dose escalation and expansion trial. *Lancet*. 2017;389(10088):2492-2502. doi:10.1016/s0140-6736(17)31046-2
40. Costa-Pinheiro P, Heher A, Raymond MH, et al. Role of SPTSSB-regulated de Novo sphingolipid synthesis in prostate cancer depends on androgen receptor signaling. *iScience*. 2020;23(12):101855. doi:10.1016/j.isci.2020.101855
41. Hage C, Hoves S, Ashoff M, et al. Characterizing responsive and refractory orthotopic mouse models of hepatocellular carcinoma in cancer immunotherapy. *PLoS One*. 2019;14(7):e0219517. doi:10.1371/journal.pone.0219517
42. Benkhoucha M, Santiago-Raber ML, Schneiter G, et al. Hepatocyte growth factor inhibits CNS autoimmunity by inducing tolerogenic dendritic cells and CD25⁺Foxp3⁺ regulatory T cells. *Proc Natl Acad Sci U S A*. 2010;107(14):6424-6429. doi:10.1073/pnas.0912437107
43. Chen S, Lai SWT, Brown CE, Feng M. Harnessing and enhancing macrophage phagocytosis for cancer therapy. *Front Immunol*. 2021;12:635173. doi:10.3389/fimmu.2021.635173
44. Kamada T, Togashi Y, Tay C, et al. PD-1⁺ regulatory T cells amplified by PD-1 blockade promote hyperprogression of cancer. *Proc Natl Acad Sci*. 2019;116(20):9999-10008. doi:10.1073/pnas.1822001116
45. Kumagai S, Togashi Y, Kamada T, et al. The PD-1 expression balance between effector and regulatory T cells predicts the clinical efficacy of PD-1 blockade therapies. *Nat Immunol*. 2020;21(11):1346-1358. doi:10.1038/s41590-020-0769-3
46. Yau T, Kang YK, Kim TY, et al. Efficacy and safety of nivolumab plus ipilimumab in patients with advanced hepatocellular carcinoma previously treated with sorafenib: the CheckMate 040 randomized clinical trial. *JAMA Oncol*. 2020;6(11):e204564. doi:10.1001/jamaoncol.2020.4564
47. Walker LS. Treg and CTLA-4: two intertwining pathways to immune tolerance. *J Autoimmun*. 2013;45:49-57. doi:10.1016/j.jaut.2013.06.006
48. Bu DX, Tarrío M, Grabie N, et al. Statin-induced Kruppel-like factor 2 expression in human and mouse T cells reduces inflammatory and pathogenic responses. *J Clin Invest*. 2010;120(6):1961-1970. doi:10.1172/JCI41384
49. Weinreich MA, Takada K, Skon C, Reiner SL, Jameson SC, Hogquist KA. KLF2 transcription-factor deficiency in T cells results in unrestrained cytokine production and upregulation of bystander chemokine receptors. *Immunity*. 2009;31(1):122-130. doi:10.1016/j.immuni.2009.05.011
50. Chen CX, Rowell EA, Thomas RM, Hancock WW, Wells AD. Transcriptional regulation by Foxp3 is associated with direct promoter occupancy and modulation of histone acetylation. *J Biol Chem*. 2006;281(48):36828-36834. doi:10.1074/jbc.M608848200

SUPPORTING INFORMATION

Additional supporting information may be found in the online version of the article at the publisher's website.

How to cite this article: Qi X, Wu F, Kim SH, et al. Nanoliposome C6-Ceramide in combination with anti-CTLA4 antibody improves anti-tumor immunity in hepatocellular cancer. *FASEB J*. 2022;36:e22250. doi:[10.1096/fj.202101707R](https://doi.org/10.1096/fj.202101707R)